

Evidence of Deformation in  $V^{51}\dagger$ 

W. SCHOLZ AND F. B. MALIK  
*Yale University, New Haven, Connecticut*

(Received 8 October 1965; revised manuscript received 28 February 1966)

The energy levels, static moments, and transition rates of  $V^{51}$  have been investigated using the strong-coupling symmetric-rotator model. Nilsson's energy levels and wave functions in the  $1f-2p$  shell are re-computed for a well depth corresponding to  $\hbar\omega_0 = 41/A^{1/2}$  MeV and for a spin-orbit strength  $C = -0.26 \hbar\omega_0$  appropriate to the  $1f-2p$  shell. The shell-model level ordering at zero deformation requires a well-flattening parameter  $D = -0.035 \hbar\omega_0$ . Band-head energies are not adjusted, but determined strictly from the appropriate summation over the occupied states. The final spectrum is obtained by diagonalizing the Coriolis coupling term with the rotational wave function based on the ten available single-particle or single-hole states in the  $1f-2p$  shell. The same moment of inertia has been used for all bands and is determined from a least-squares fit to the experimental level scheme. Both for a deformation parameter  $\beta = -0.32$  and for  $\beta = 0.20$ , the calculated spectrum is in reasonable agreement with the experiment. The rotational bands are mixed to a high degree. As a consequence the band structure is destroyed and the lowest eigenvalue of the spectrum becomes  $\frac{1}{2}$ . The wave functions corresponding to the optimal deformation are used in predicting (a) the magnetic moment of the ground and the first excited state, (b) the ground-state quadrupole moment, and (c) the magnetic dipole and the electric quadrupole transition probabilities. The agreement with the experiment, especially for the oblate deformation, is good and is achieved without using an effective charge and an effective gyromagnetic ratio.

## I. INTRODUCTION

IN recent years many attempts<sup>1-9</sup> have been made to study the properties of nuclei in the  $1f_{7/2}$  shell in terms of the spherical shell model with a suitable residual interaction between nucleons in a  $(1f_{7/2})^n$  configuration outside the closed shells. In particular, the work of McCullen, Bayman, and Zamick<sup>1</sup> has elucidated a number of properties of these nuclei to a certain extent but has also raised a number of questions on the behavior of odd nuclei in this region of the periodic table. In spite of the relative paucity of experimental information on the odd nuclei in this mass region, disagreement between theory and observation becomes evident on a number of important points, as noted previously<sup>1</sup> and as summarized below:

(a) The cross conjugate pairs of nuclei, e.g.,  $Ti^{47}$  and  $V^{49}$ , do not exhibit the same excitation spectrum even with regard to the lowest few levels as expected from the above shell-model computations.

(b) The equivalent pairs, i.e., the nuclei having the same number of particles and holes, are predicted to have approximately the same level spectrum according to this shell model. Although extensive experimental information is as yet not available, there appears to be

disagreement between the low-lying spectra of  $Ca^{43}$ ,  $Ca^{45}$ ,  $V^{51}$ , and  $Mn^{53}$ .

(c) The most remarkable disagreement concerns the level densities in the low-excitation energy region, e.g., in  $Sc^{45}$  ten levels below 1.6 MeV have been observed whereas only one is expected from the shell-model calculation mentioned above.<sup>1</sup>

While these discrepancies may not appear immediately relevant to a discussion of  $V^{51}$ , they emphasize the inherent difficulties in a pure  $(1f_{7/2})^n$  shell-model treatment for odd nuclei in this mass region including  $V^{51}$ .

$V^{51}$  is the *only* odd nucleus in the  $1f_{7/2}$  shell which has sufficient experimental data for a more detailed theoretical study. While the shell model predicts the location of the first four energy levels with reasonable accuracy, the following discrepancies are worth further consideration:

(i) The computed  $B(E2)$  transition rates are typically an order of magnitude slower than the observed ones throughout the  $1f_{7/2}$  shell. This has been reflected in the use of an unusually high effective charge between 2.0 and 2.5<sup>5,8,9</sup> for each of the three  $1f_{7/2}$  protons in the shell model of  $V^{51}$ . The observed quadrupole moment,<sup>10</sup> on the other hand, is somewhat smaller than the single-particle moment and requires an effective charge of unity or less to parametrize this in terms of the shell model.

(ii) The only energy level in the 2.0- to 3.0-MeV range of excitation energy in the shell-model treatment based on a  $(1f_{7/2})^3$  configuration is a  $15/2^-$  state. Four states are observed in this region,<sup>11</sup> of which two are strongly excited in  $(pp')$  scattering,<sup>12</sup> whereas this would not be expected for a state with spin  $15/2$ .

<sup>†</sup> Work supported in part by the U. S. Atomic Energy Commission under Contract No. AT(30-1)-3223 and the National Science Foundation.

<sup>1</sup> J. D. McCullen, B. F. Bayman, and L. Zamick, *Phys. Rev.* **134**, B515 (1964).

<sup>2</sup> R. D. Lawson and J. L. Uretsky, *Phys. Rev.* **106**, 1369 (1957).

<sup>3</sup> A. R. Edmonds and B. H. Flowers, *Proc. Roy. Soc. (London)* **A215**, 120 (1952).

<sup>4</sup> D. Kurath, *Phys. Rev.* **91**, 1430 (1953).

<sup>5</sup> H. W. Kendall and I. Talmi, *Phys. Rev.* **128**, 792 (1962).

<sup>6</sup> B. F. Bayman, J. D. McCullen, and L. Zamick, *Phys. Rev. Letters* **11**, 215 (1963).

<sup>7</sup> J. Vervier, *Phys. Letters* **5**, 79 (1963).

<sup>8</sup> J. Vervier, *Phys. Letters* **13**, 47 (1964).

<sup>9</sup> L. Zamick and J. D. McCullen, *Bull. Am. Phys. Soc.* **10**, 485 (1965).

<sup>10</sup> H. Nagasawa, S. K. Takeshita, and Y. Tomono, *J. Phys. Soc. (Japan)* **19**, 764 (1964).

<sup>11</sup> J. E. Schwäger, *Phys. Rev.* **121**, 569 (1961).

<sup>12</sup> H. O. Funsten, N. R. Robertson, and E. Rost, *Phys. Rev.* **134**, B117 (1964).

In view of these discrepancies, it is natural to look for alternative descriptions of the properties of  $V^{51}$ . Attempts have been made to describe the properties of  $V^{51}$  within the framework of the weak-coupling model<sup>13</sup> but without clarifying the above mentioned difficulties (see Ref. 5). The superfluid model computation of Kisslinger and Sorensen<sup>14</sup> does not reproduce the level spectrum. Lawson<sup>15</sup> applied Hill and Wheeler's<sup>16</sup> method of generator coordinates to odd nuclei in the  $1f_{7/2}$  shell. In his work, no attempt was made to obtain the level spectrum and the transition rates of  $V^{51}$ . Our treatment applying the model of Bohr and Mottelson<sup>17</sup> with strong Coriolis coupling between rotational bands differs from that of Lawson in a number of aspects including the following: (a) Nilsson's<sup>18</sup> single-particle orbitals have been recomputed using a spin-orbit coupling strength appropriate to the  $1f_{7/2}$  shell. (b) A static deformation has been used instead of the  $\beta \approx 0$  case considered by Lawson. (c) Coriolis coupling between different bands has been considered explicitly. (d) All single-particle and hole states available in the  $N=3$  shell have been included in diagonalizing the Coriolis coupling.

## II. THE MODEL

The basic approach in the present treatment involves the strong-coupling collective model suggested by Bohr and Mottelson.<sup>17</sup> In this model all but the last odd nucleon are incorporated in the deformed core. This deformed core has angular momentum  $\mathbf{R}$  and the total model Hamiltonian is given by

$$H = \frac{\hbar^2}{2\mathcal{J}_x} R_x^2 + \frac{\hbar^2}{2\mathcal{J}_y} R_y^2 + \frac{\hbar^2}{2\mathcal{J}_z} R_z^2 + H_p, \quad (1)$$

where the first three terms describe the core rotation and  $H_p$  represents the single-particle motion with respect to the core in the body-fixed coordinates.  $\mathcal{J}_x$ ,  $\mathcal{J}_y$ , and  $\mathcal{J}_z$  and  $R_x$ ,  $R_y$ , and  $R_z$  are, respectively, the Cartesian components of the moment of inertia  $\mathcal{J}$ , and the angular momentum  $\mathbf{R}$  in this coordinate system. For a deformation symmetric relative to the  $z$  axis  $\mathcal{J}_x = \mathcal{J}_y = \mathcal{J}$  and the Hamiltonian may be expressed in terms of the total angular momentum  $\mathbf{I}$

$$H = (\hbar^2/2\mathcal{J})(\mathbf{I}^2 + \mathbf{j}^2 - 2(\mathbf{I} \cdot \mathbf{j})) + H_p, \quad (1)$$

where

$$\mathbf{I} = \mathbf{R} + \mathbf{j} \quad (2)$$

and  $\mathbf{j}$  is the intrinsic angular momentum operator.

The Coriolis term  $\mathbf{I} \cdot \mathbf{j}$  couples the particle motion to the core rotation. In the following sections we first discuss the particle motion, then the core rotation, and finally the coupling of the two.

### A. The Single-Particle Aspect

The interaction between the last nucleon and the core may be represented by an effective anisotropic harmonic oscillator potential as suggested by Nilsson.<sup>18</sup> The Hamiltonian of the last odd nucleon is

$$H_p = -(\hbar^2/2\mu)\Delta + (1/2)\mu(\omega_\rho^2 x^2 + \omega_\rho^2 y^2 + \omega_z z^2) + C\mathbf{l} \cdot \mathbf{s} + D\mathbf{l} \cdot \mathbf{I}, \quad (3)$$

where  $\mu$  is the reduced mass of the last nucleon,  $C$  is the strength of the average spin-orbit splitting in the  $1f_{7/2}$  shell, and  $D$  serves to depress the states with higher orbital angular momentum. The anisotropy is assumed to have rotational symmetry about the  $z$  axis, hence the frequency in the  $x$ - or  $y$ -direction each equals  $\omega_\rho$ ;  $\omega_z$  is the oscillator frequency in the  $z$ -direction. Because of this anisotropy, the projection  $\Omega$  of the angular momentum  $\mathbf{j}$  on the axis of the symmetry—and not  $\mathbf{j}$  itself—is a good quantum number.

It is convenient to introduce the transformation

$$\xi = x(\mu\omega_\rho/\hbar)^{1/2}; \quad \eta = y(\mu\omega_\rho/\hbar)^{1/2}; \quad \zeta = z(\mu\omega_z/\hbar)^{1/2} \quad (4)$$

and express the frequencies in terms of a parameter  $B$ ,<sup>19</sup>

$$\begin{aligned} \omega_\rho &= \omega_0(B)(1 + \frac{1}{2}B), \\ \omega_z &= \omega_0(B)(1 - B), \end{aligned} \quad (5)$$

where  $B$  is related to the standard deformation parameter  $\beta$  by the following relation:

$$B = 2c(2-c)/(4-c^2), \quad \text{where } c = (5/4\pi)^{1/2}\beta. \quad (6)$$

The constraint of the volume conservation relates  $\omega_0(B)$  to  $\omega_0(0)$ , the corresponding frequency for zero deformation, by

$$\hbar\omega_0(B) = \hbar\omega_0(0)[1 - \frac{3}{4}B^2 - \frac{1}{4}B^3]^{-1/3}. \quad (7)$$

Equation (3) may be written as

$$H_p = \frac{1}{2}\hbar\omega_0(B)[-d^2/d\xi^2 + 2\xi^2 - d^2/d\eta^2 + 2\eta^2 - d^2/d\zeta^2 + 2\zeta^2] - \hbar\omega_0(B)(4\pi/5)^{1/2}B\rho^2 Y_{2,0}(\theta, \varphi) + C\mathbf{l} \cdot \mathbf{s} + D\mathbf{l} \cdot \mathbf{I}, \quad (8)$$

where  $\rho^2 = \xi^2 + \eta^2 + \zeta^2$  and  $Y_{2,0}(\theta, \varphi)$  is the normalized spherical harmonics.

As noted by Nilsson,  $\mathbf{l}$  and  $\mathbf{s}$  in (8) are in principle different from those in (3) but an estimate shows that this difference in  $\mathbf{l}$  is of the order of 2% for  $\beta = 0.4$  and in consequence it is neglected here.

The eigenfunctions of  $H_p$  may be written as

$$\chi_{\Omega, \nu} = \sum_j c_{j, \Omega, \nu} |j\Omega\rangle \quad (9a)$$

<sup>19</sup> T. D. Newton, Can. J. Phys. 38, 700 (1960).

<sup>13</sup> A. de Shalit, *Selected Topics in Nuclear Theory*, edited by F. Janouch (International Atomic Energy Commission, Vienna, 1963), p. 209.

<sup>14</sup> L. S. Kisslinger and R. A. Sorensen, Kgl. Danske Videnskab. Selskab. Mat. Fys. Medd. 32, No. 9 (1960).

<sup>15</sup> R. D. Lawson, Phys. Rev. 124, 1500 (1961).

<sup>16</sup> D. Hill and J. A. Wheeler, Phys. Rev. 89, 1102 (1953).

<sup>17</sup> A. Bohr and B. R. Mottelson, Kgl. Danske Videnskab. Selskab. Mat. Fys. Medd. 27, No. 16 (1953).

<sup>18</sup> S. G. Nilsson, Kgl. Danske Videnskab. Selskab. Mat. Fys. Medd. 29, No. 16 (1955).

and for the negative projection

$$\chi_{-\Omega, \nu} = \sum_j (-1)^{j-1/2} c_{j, \Omega, \nu} |j-\Omega\rangle, \quad (9b)$$

where  $|j\Omega\rangle$  are the wave functions of the unperturbed oscillator Hamiltonian. The extra index  $\nu$  has been introduced to distinguish among different Nilsson levels in the same oscillator shell with the same projection quantum number  $\Omega$ .

The expansion coefficients  $c_{j, \Omega, \nu}$  and the eigenvalues  $E_{\Omega, \nu}$  are obtained by diagonalizing the single-particle Hamiltonian.

Assuming that the Nilsson single-particle energies are derived from the basic two-nucleon potential, the total energy of the system is not the sum of the single-particle energies but given by the following expression:

$$E = \sum \frac{1}{2}(1 + \mu/2M)E_{\Omega, \nu} - (\mu/4M)(\mathbf{C}\mathbf{l} \cdot \mathbf{s} + D\mathbf{l} \cdot \mathbf{l}), \quad (10)$$

where  $E_{\Omega, \nu}$  is the Nilsson energy of individual nucleons and  $M$  is the nucleonic mass and the summation runs over all occupied levels.

Excited particle states have been constructed by lifting the last unpaired nucleon to any one of the higher unoccupied levels; similarly hole states or core excited states have been generated by lifting a core particle and pairing it with the odd nucleon. Under the assumption that the pairing energy within the same oscillator shell does not depend on the occupied Nilsson level, the energy of the hole state and its eigenfunction are also obtained from (10) and (9), respectively. (Other types of hole states obtained by lifting a core particle to any state other than that occupied by the odd nucleon or by lifting more than one core particle are not considered herein).

### B. Rotational Motion and Coriolis Coupling

The eigenfunctions of the operator  $(\hbar^2/2g)\mathbf{I}^2$  are the normalized  $D$  functions. In the absence of the Coriolis coupling  $\mathbf{I} \cdot \mathbf{j}$ , the total wave function  $\Phi$  is a properly symmetrized product of the  $D$  function, the single-particle function  $\chi_{\Omega, \nu}$ , and the wave function of the core  $\varphi_c$

$$\Phi = \left(\frac{2I+1}{16\pi^2}\right)^{1/2} [D_{MK}^I(\theta)\chi_{\Omega, \nu} + (-1)^{I-1/2}D_{M-K}^I(\theta)\chi_{-\Omega, \nu}]\varphi_c, \quad (11)$$

where  $K$  is equal to  $\Omega$  for a symmetric rotator.

$\Phi$  is not an adequate wave function when the Coriolis interaction is included in the model Hamiltonian; how-

ever, we may use  $\Phi$  as a suitable basis and expand the total wave function

$$\Psi(I, M) = \left(\frac{2I+1}{16\pi^2}\right)^{1/2} \sum_{K=\Omega} \sum_{\nu} C_{K, \nu} [D_{MK}^I(\theta)\chi_{\Omega, \nu} + (-1)^{I-1/2}D_{M-K}^I(\theta)\chi_{-\Omega, \nu}]\varphi_c, \quad (12)$$

where the summation extends from the allowed positive to the negative values of  $K$  in steps of two. The coefficients  $C_{K, \nu}$  are determined by the Jacobi diagonalization procedure. In this representation the Coriolis coupling connects states  $|\Delta K| = \pm 1$  and  $\Delta K = 0$  for  $K = \frac{1}{2}$  band. The diagonal and off-diagonal matrix elements are given by the following expressions

$$\langle IMK\nu | H(D) | IMK\nu \rangle = (\hbar^2/2g)[I(I+1) - K^2 - \Omega^2], \quad (13)$$

$$\begin{aligned} &\langle IMK\nu_1 | H(OD) | IM-(K\pm 1)\nu_2 \rangle \\ &= -(\hbar^2/2g)\{[(I\mp K)(I\pm K+1)]^{1/2} \\ &\quad \times \sum_j c_{j, \Omega, \nu_1} c_{j, -( \Omega \pm 1), \nu_2} (-1)^{I-j} [(j\mp \Omega)(j\pm \Omega+1)]^{1/2} \\ &\quad + \sum_j c_{j, \Omega, \nu_1} c_{j, \Omega, \nu_2} j(j+1)\}, \quad (14) \end{aligned}$$

where  $H(D)$  and  $H(OD)$  are, respectively, the diagonal and the off-diagonal part of the model Hamiltonian (1) with respect to the chosen basis (11).

The matrix elements (13) and (14) are written with the specific assumption that the core wave function  $\varphi_c$  does not depend on  $K$ ,  $j$ ,  $\nu$ , or  $\Omega$ . This assumption, although reasonable, is only valid for a rigid core. The other assumption is the scalar nature of the moment of inertia operator.

If the Coriolis coupling is strong in comparison with the single-particle energy spacing, the ground-state spin is not known *a priori*. However the ground-state spin is uniquely determined to be the spin associated with the lowest eigenvalue obtained after the diagonalization. The complete level spectrum and the associated spins are given by the spin and the magnitude of the successive eigenvalues.

### C. Moments

The magnetic and electric moment tensors may be transformed to the body-fixed coordinates with the respective irreducible representations. Moments corresponding to a particular state of spin  $I$  are then computed with the corresponding wave function (12). Thus the magnetic moment  $\mu(I)$  is given by

$$\begin{aligned} \mu(I) = &g_R I + [1/(I+1)] \sum_{K, \nu_i, \nu_f} C_{K, \nu_i} C_{K, \nu_f} K [(g_s - g_l)\langle s_0 \rangle + (g_l - g_R)\langle j_0 \rangle] \\ &+ \sum_{K, \nu_i, \nu_f} C_{K, \nu_i} C_{-K+1, \nu_f} (-1)^{I-1/2} (I1K-1 | IK-1) [(g_s - g_l)\langle s_- \rangle + (g_l - g_R)\langle j_- \rangle] / \sqrt{2} \\ &+ \sum_{K, \nu_i, \nu_f} C_{K, \nu_i} C_{-K-1, \nu_f} (-1)^{I+1/2} (I1K1 | IK+1) [(g_s - g_l)\langle s_+ \rangle + (g_l - g_R)\langle j_+ \rangle] / \sqrt{2}, \quad (15) \end{aligned}$$

where in our convention the summation runs from the positive to the negative values of  $K$  in steps of two.  $g_l$ ,  $g_s$ , and  $g_R$  are the orbital, the intrinsic, and the core gyromagnetic ratio, respectively.

Moreover,

$$\begin{aligned}
\langle j_0 \rangle &= \sum_j \Omega c_{j,\Omega,\nu_i} c_{j,\Omega,\nu_f}, \\
\langle j_+ \rangle &= \sum_j (-1)^{j-1/2} (j-\Omega)^{1/2} (j+\Omega+1)^{1/2} c_{j,\Omega=K,\nu_i} c_{j,\Omega=-K-1,\nu_f}, \\
\langle j_- \rangle &= \sum_j (-1)^{j-1/2} (j+\Omega)^{1/2} (j-\Omega+1)^{1/2} c_{j,\Omega=K,\nu_i} c_{j,\Omega=-K+1,\nu_f}, \\
\langle s_0 \rangle &= \frac{1}{2} \sum_l (a_{l,\Omega-1/2,1/2,\nu_i} a_{l,\Omega-1/2,1/2,\nu_f} - a_{l,\Omega+1/2,-1/2,\nu_i} a_{l,\Omega+1/2,-1/2,\nu_f}), \\
\langle s_+ \rangle &= \sum_l (-1)^l a_{l,\Omega+1/2,-1/2,\nu_i} a_{l,-(\Omega+1/2),-1/2,\nu_f}, \\
\langle s_- \rangle &= \sum_l (-1)^l a_{l,\Omega-1/2,1/2,\nu_i} a_{l,-(\Omega-1/2),1/2,\nu_f},
\end{aligned} \tag{16}$$

where the Nilsson coefficients  $a_{l,\Lambda,\Sigma,\nu}$  are related to  $c_{j,\Omega,\nu}$  by

$$a_{l,\Lambda,\Sigma,\nu} = \sum_j \left( \frac{1}{2} l \Sigma \Lambda \mid j \Omega \right) c_{j,\Omega,\nu}. \tag{17}$$

The quadrupole moment  $Q$  of a state of spin  $I$  is given by

$$Q = Q_{\text{coll}} + (I2I0 \mid II) (q(0) + q(2) + q(-2)), \tag{18}$$

where the collective contribution to the quadrupole moment is

$$Q_{\text{coll}} = Q_0 \sum_{K,\nu} |C_{K,\nu}|^2 \frac{3K^2 - I(I+1)}{(I+1)(2I+3)} \tag{19}$$

and the intrinsic moment of the core to second order in  $\beta$  is

$$Q_0 = [3/\sqrt{5\pi}] e(Z-1) R^2 \beta (1 + 0.16\beta). \tag{20}$$

The terms  $q(0)$ ,  $q(2)$ , and  $q(-2)$  are the single-particle contributions to the quadrupole moment and are defined by

$$\begin{aligned}
q(n) &= (-1)^{n(I_f-1/2)} (2e_p \hbar / M \omega_0) \sum_{K,\nu_i,\nu_f} (I_i 2K n \mid I_f K + n) C_{K,\nu_i} C_{(-1)^n(K+n),\nu_f} \\
&\times \left\{ \sum_{l,\Lambda,\Sigma} [(l200 \mid l0) (l2\Lambda n \mid l\Lambda + n) (N+3/2) a_{l,\Lambda,\Sigma,\nu_i} a_{l,\Lambda',\Sigma',\nu_f} + (l200 \mid l-20) (l2\Lambda n \mid l-2\Lambda + n) \right. \\
&\times [(2l+1)/(2l-3)]^{1/2} [(N-l+2)(N+l+1)]^{1/2} a_{l,\Lambda,\Sigma,\nu_i} a_{l-2,\Lambda',\Sigma',\nu_f} + (l200 \mid l+20) (l2\Lambda n \mid l+2\Lambda + n) \\
&\left. \times [(2l+1)/(2l+5)]^{1/2} [(N-l)(N+l+3)]^{1/2} a_{l,\Lambda,\Sigma,\nu_i} a_{l+2,\Lambda',\Sigma',\nu_f} \right\} \text{ for } n=0, \pm 1, \pm 2, \tag{21}
\end{aligned}$$

where  $i$  and  $f$  refer to the initial and the final states,  $\Lambda' = (-1)^n(\Lambda+n)$  and  $\Sigma' = (-1)^n\Sigma$ . For the quadrupole moment,  $i=f$  and  $I_i=I_f$ .

#### D. Transition Rates

The  $\lambda$ -multipole transition probability is given by

$$T(\lambda; i \rightarrow f) = \frac{8\pi(\lambda+1)}{\lambda[(2\lambda+1)!!]^2} \frac{1}{\hbar} \left( \frac{E}{\hbar c} \right)^{2\lambda+1} B(\lambda; i \rightarrow f), \tag{22}$$

where  $B(\lambda; i \rightarrow f)$  is the reduced transition rate.

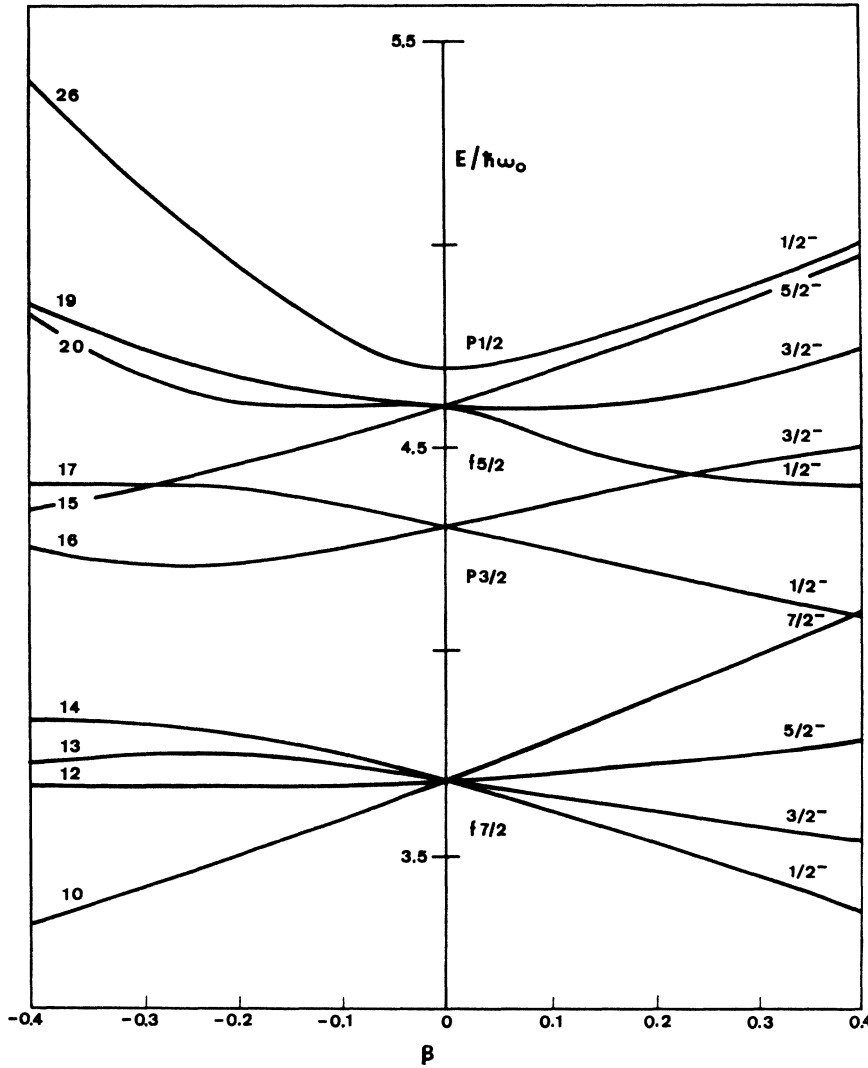


FIG. 1. Single-particle eigenvalues in the  $1f-2p$  shell as a function of the deformation parameter  $\beta$  in units of  $\hbar\omega_0$  for a spin-orbit strength  $C = -0.26\hbar\omega_0$  and a well-flattening parameter  $D = -0.035\hbar\omega_0$ . The integers adjacent to the levels indicate the associated Nilsson orbit number. The levels are identified at zero deformation via spherical shell model notation and at nonzero deformation by the values of  $\Omega$  and the parity for the orbit.

For the  $M1$  transition, the reduced transition probability is given by

$$\begin{aligned}
 B(M1; i \rightarrow f) = & \frac{3}{4\pi} [g_R(I_i(I_i+1))]^{1/2} \delta_{I_i I_f} \sum_{K, \nu_i, \nu_f} C_{K, \nu_i} C_{K, \nu_f} + \sum_{K, \nu_i, \nu_f} C_{K, \nu_i} C_{K, \nu_f} (I_i 1 K 0 | I_f K) \\
 & \times [(g_s - g_l) \langle s_0 \rangle + (g_l - g_R) \langle j_0 \rangle] + \sum_{K, \nu_i, \nu_f} C_{K, \nu_i} C_{-K+1, \nu_f} (-1)^{I_f - 1/2} (I_i 1 K - 1 | I_f K - 1) \\
 & \times [(g_s - g_l) \langle s_- \rangle + (g_l - g_R) \langle j_- \rangle] / \sqrt{2} + \sum_{K, \nu_i, \nu_f} C_{K, \nu_i} C_{-K-1, \nu_f} (-1)^{I_f + 1/2} \\
 & \times (I_i 1 K + 1 | I_f K + 1) [(g_s - g_l) \langle s_+ \rangle + (g_l - g_R) \langle j_+ \rangle] / \sqrt{2} \quad (23)
 \end{aligned}$$

The symbols are defined in (16) and (17).

The reduced electric quadrupole transition rate  $B(E2; i \rightarrow f)$  is given by

$$\begin{aligned}
 B(E2; i \rightarrow f) = & (5/16\pi) \\
 & \times [Q_e + q(0) + q(1) + q(-1) + q(2) + q(-2)]^2, \quad (24)
 \end{aligned}$$

where the collective contribution

$$Q_e = Q_0 \sum_{K, \nu_i, \nu_f} C_{K, \nu_i} C_{K, \nu_f} (I_i 2 K 0 | I_f K). \quad (25)$$

The remaining symbols are defined in Eqs. (16)–(21). Similar expressions for the case of asymmetric deforma-

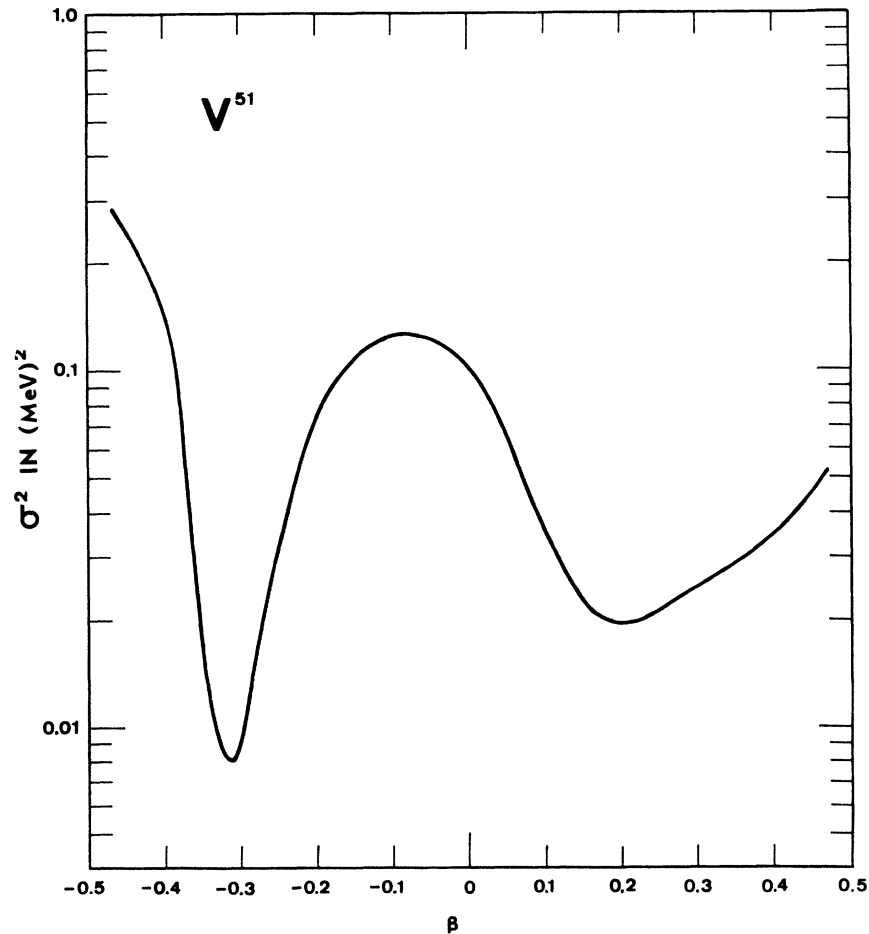


FIG. 2. Mean-squared deviation between the computed and the experimental level position of the  $\frac{7}{2}^-$ ,  $\frac{9}{2}^-$ ,  $11/2^-$ , and  $\frac{13}{2}^-$  state as a function of the deformation. The rotational constant  $A = \hbar^2/2\mathcal{I}$  is optimized at each value of  $\beta$ .  $A = 273$  keV and 233 keV at  $\beta = -0.32$  and  $\beta = 0.2$ , respectively.

tions have been derived previously by Hecht and Satchler<sup>20</sup> for one single-particle level and by Chi and Davidson<sup>21</sup> for many single-particle levels.

### III. DETAILS OF THE CALCULATION

In our calculations we have chosen the usual value of  $\hbar\omega_0 = 41/A^{1/3}$  MeV for the energy of the oscillator quantum. This choice is consistent with the separation energy of the last proton in  $V^{51}$ . The nuclear radius  $R$  is given as usual by  $R = 1.2A^{1/3}$  F. The observed spin-orbit splitting between the  $1f_{7/2}$  and  $1f_{5/2}$  levels in  $Ca^{41}$  yields  $C = -0.26\hbar\omega_0$  as the strength of the spin-orbit interaction; a well-flattening parameter  $D = -0.035\hbar\omega_0$  has been chosen to preserve the shell-model level ordering at zero deformation (Fig. 1). The deformation parameter  $\beta$  and *only one* rotational constant  $A = \hbar^2/2\mathcal{I}$  for all bands are used as free parameters in the calculation and are determined by a least-squares fit to the experimental level spectrum (Fig. 2). In this connection it is interesting to point out that the value of  $A$  obtained finally from the least-squares fit is consistent with the

excitation energy of the first  $2^+$  state in adjacent even-even nuclei assuming a rotational character for this state.

In the band mixing calculation we have included all bands in the  $1f-2p$  shell which are coupled by the Coriolis interaction to the band based on the lowest possible intrinsic state with one unpaired proton in Nilsson level 13 or 12 for positive or negative deformation, respectively. In addition, eight bands based on excited intrinsic particle states are obtained by lifting this unpaired proton to the higher Nilsson levels. One band based on a hole or core excited state arises from lifting one proton from Nilsson level 14 or 10 and pairing it with the odd proton on Nilsson level 13 or 12 for positive and negative deformation, respectively. Single-particle states obtained by excitation of the closed neutron shell are not coupled by the Coriolis interaction to the bands mentioned above. In addition, as can be inferred from the observed energy gap in neighboring even-even nuclei such states are not expected below about 3 MeV in the level spectrum and have therefore not been included in our treatment. With the additional assumption that the pairing energy does not depend on the occupied Nilsson level, expression

<sup>20</sup> K. T. Hecht and G. R. Satchler, Nucl. Phys. **32**, 286 (1962).

<sup>21</sup> B. E. Chi and J. P. Davidson, Phys. Rev. **131**, 366 (1963).

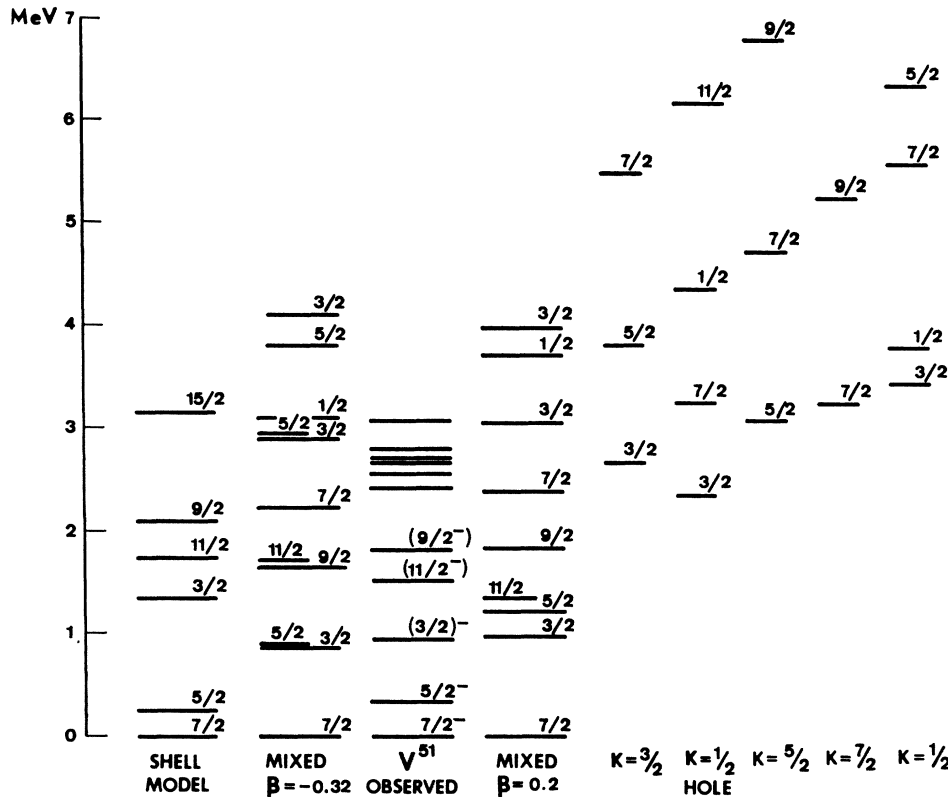


FIG. 3. Experimental energy levels of  $V^{51}$  and the level spectrum calculated in the Coriolis coupling model for  $\beta = -0.32$  and  $\beta = 0.20$ . The five columns on the right indicate the unperturbed level positions of the lowest five bands for  $\beta = 0.20$ . The remaining five bands included in the band mixing calculation are not important for the lower excitation region and are not shown. The leftmost column shows the shell-model computation taken from Ref. 1.

(10) completely determines the single-particle energies. No adjustment of the band-head energies is made in our computation. Matrix elements of the Coriolis coupling are computed from expressions (13) and (14) using our single-particle wave functions. The Coriolis coupling does not connect a hole and an excited-particle state. The final spectrum and wave functions are obtained by diagonalizing the Coriolis coupling term with the rotational wave function based on the ten available single-particle or single-hole levels in the  $1f-2p$  shell.

Moments and transition rates are computed using the free proton charge of unity and the free gyromagnetic ratio. A rotational  $g$  factor of  $Z/A$  has been used.

IV. RESULTS AND DISCUSSION

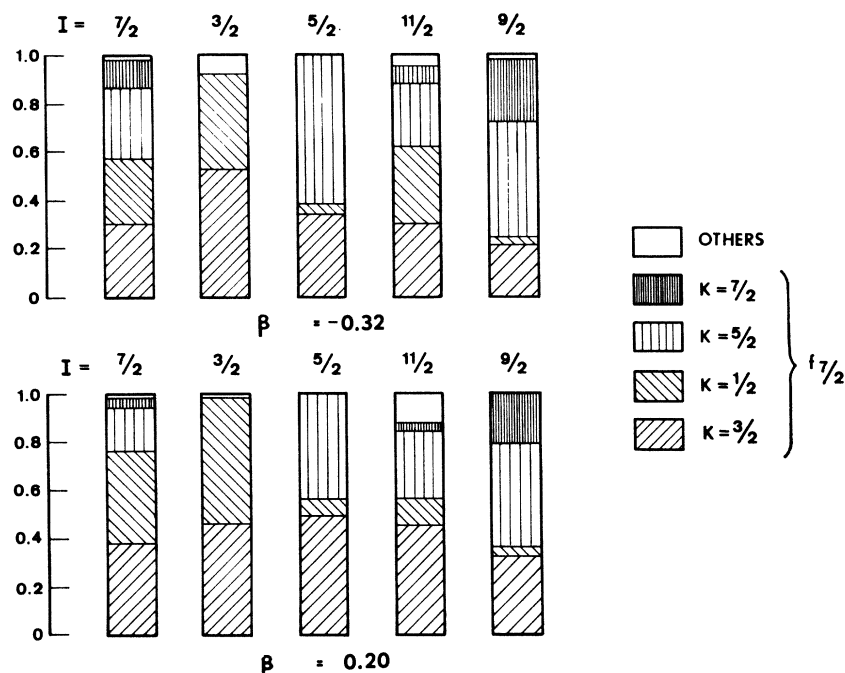
The least-squares fit to the experimental energy levels (Fig. 2) shows one pronounced and one more shallow minimum at  $\beta = -0.32$  and  $+0.20$ , respectively. The level spectra calculated for these values of  $\beta$  are shown in Fig. 3 along with the shell-model fit<sup>1</sup> and the experimental level scheme. The close similarity of the two level schemes computed for positive and negative deformation emphasizes the relative insensitivity to minor changes in band-head energies and shows that the final spectrum is determined to a large extent by the strong Coriolis coupling present between states with high spin  $I$  and low projection quantum number  $K$ . This strong Coriolis coupling together with the large negative decoupling factor  $a \approx -3.7$  for Nilsson level 14

(see Fig. 3) is responsible for the occurrence of a  $\frac{7}{2}^-$  ground-state spin. Therefore, this fact may not be interpreted as evidence in favor of the shell model as has been done until now. Apart from the  $\frac{5}{2}^-$  first excited state the agreement with the experimental level positions is quite satisfactory. It is worth mentioning that the position of the  $\frac{5}{2}^-$  state can be depressed by using a smaller rotational constant at the expense of the agreement with the higher levels. The mean-square deviation of the calculated level energies for the first four excited states is the same for both the shell model and the strong-coupling model. Two additional levels observed in inelastic proton scattering,<sup>12</sup> presumably negative-parity states with spin  $\frac{3}{2} \leq I \leq 11/2$ , may correspond to the  $\frac{7}{2}^-$  and  $\frac{3}{2}^-$  states predicted between 2 and 3 MeV. These two states cannot be obtained in the shell-model calculation restricted to the  $(f_{7/2})^3$  configuration.

Because of the strong Coriolis coupling, the band mixing in  $V^{51}$  is very pronounced (Fig. 4). As a consequence the collective contribution to the computed quadrupole moment as given by expression (19) is reduced from the intrinsic quadrupole moment  $Q_0 = 0.71$  and  $-1.04$  b for  $\beta = 0.20$  and  $-0.32$  to  $Q_{\text{coll}} = -0.12$  and  $0.04$  b, respectively, and the single-particle contribution becomes significant and has to be taken into account (Fig. 5). The absolute magnitude of the quadrupole moment has been measured as  $|Q| = 0.0073$  b.<sup>22,10</sup>

<sup>22</sup> The antishielding factor  $\gamma$  used to extract  $Q$  from the experiment is uncertain, which makes it difficult to estimate the error in  $Q$ .

FIG. 4. The squared band mixing amplitudes  $|C_{K,\nu}|^2$  for the lowest five eigenstates. Contributions of bands with parentage other than  $f_{7/2}$  are small and not given separately.



Although the agreement with experiment is much better for negative deformation, the large cancellation in the collective contribution to the quadrupole moment, which is sensitive to small changes in the wave function, precludes any final conclusion with regard to the sign of the deformation. The quadrupole moment given by the shell model with the  $(1f_{7/2})^3$  configuration mixture<sup>23</sup> is too large. It should also be noted that an effective charge of about two, which is required to explain the  $B(E2)$  enhancement, will increase the discrepancy.

Figure 5 shows also the magnetic moments of the ground and the first excited state. Both the shell-model values and the Coriolis coupling model results are given without using effective moments. The importance of a proper inclusion of the band mixing in the formula for the magnetic moment can be seen from the contributions of the four main terms in expression (15) separately, e.g., for  $\beta = -0.32$  they contribute 1.58, 1.00, 1.55, and 1.50 nm, respectively, for the ground state.

One of the most interesting features of the experimental data related to  $V^{51}$  is the large enhancement of the  $B(E2)$  transition rates. The experimental  $B(E2)$  rates given in Fig. 6 are taken from Ref. 5, and are in agreement with the results of other workers.<sup>24,25</sup> A different value of  $B(E2; \frac{7}{2} \rightarrow \frac{3}{2}) = 0.38 \times 10^{-2} e^2 b^2$  has also been measured.<sup>26</sup> As pointed out by Kendall and Talmi<sup>5</sup> even the use of a simple effective charge of about

two for each of the three  $f_{7/2}$  shell protons in the shell model cannot account for all three transitions. On the other hand, the predictions of the deformed core model are in reasonable agreement with experiment for both positive and negative deformation.

In the shell-model  $M1$  transitions between states of the  $(1f_{7/2})^3$  configuration are forbidden by the seniority selection rule.<sup>27</sup> Observed  $M1$  transitions in  $V^{51}$  are weak. The  $M1$ -transition probability between the  $\frac{5}{2}^-$  and the  $\frac{7}{2}^-$  ground state can be deduced from the total radiation width and the  $E2/M1$  mixing ratio<sup>28</sup> as  $B(M1; \frac{5}{2}^- \rightarrow \frac{7}{2}^-) = 0.0053 \text{ nm}^2$ . Further, the observed branching ratios for the decay of the  $\frac{3}{2}^-$  and the  $\frac{9}{2}^-$  state to the  $\frac{7}{2}^-$  ground state and the  $\frac{5}{2}^-$  first excited state are 84:16 and 78:22, respectively.<sup>29</sup> Using the calculated  $B(E2)$  rates for the pure  $E2$  transitions this implies  $B(M1; \frac{3}{2}^- \rightarrow \frac{5}{2}^-) \lesssim 0.004 \text{ nm}^2$  and  $B(M1; \frac{9}{2}^- \rightarrow \frac{7}{2}^-) \lesssim 0.03 \text{ nm}^2$ . The strong-coupling model can account for the retardation in the  $M1$  transitions to the  $\frac{7}{2}^-$  ground state. The values calculated for  $\beta = -0.32$  and  $0.20$  are  $B(M1; \frac{5}{2}^- \rightarrow \frac{7}{2}^-) = 3.6 \cdot 10^{-5}$  and  $0.21 \text{ nm}^2$  and  $B(M1; \frac{9}{2}^- \rightarrow \frac{7}{2}^-) = 0.037$  and  $0.035 \text{ nm}^2$ , respectively. The experimental values can be reproduced with very small change in the wave functions because of the near cancellation among the four main terms in the bracket of expression (23), e.g., for  $\beta = -0.32$  and  $\frac{5}{2}^- \rightarrow \frac{7}{2}^-$  transition the individual contributions of the terms in the bracket are 0.000, 1.095,  $-0.719$ , and  $-0.372 \text{ nm}$ , respectively. Again negative deformation seems to be favored slightly. The computed  $M1$ -transition probability for the  $\frac{3}{2}^- \rightarrow \frac{5}{2}^-$

<sup>23</sup> J. P. Elliot and A. M. Lane, *Handbuch der Physik*, edited by S. Flügge (Springer-Verlag, Berlin, 1957), Vol. 39, p. 241.

<sup>24</sup> B. M. Adams, D. Eccleshall, and M. J. L. Yates, in *Proceedings of the Second Conference on Reactions Between Complex Nuclei*, edited by A. Zucker, E. C. Halbert, and F. T. Howard (John Wiley & Sons, Inc., New York, 1960), p. 95.

<sup>25</sup> I. Kh. Lemberg, see Ref. 24, p. 112.

<sup>26</sup> See, however, footnote "e" to Table IV in Ref. 5.

<sup>27</sup> C. Noack, *Phys. Rev.* **132**, 1213 (1963).

<sup>28</sup> R. C. Ritter, P. H. Stelson, F. K. McGowan, and R. L. Robinson, *Phys. Rev.* **128**, 2320 (1962).

<sup>29</sup> A. W. Barrows, Ph.D. thesis, University of Kentucky, 1965 (unpublished).



transition is too large.  $B(M1; \frac{3}{2}^- \rightarrow \frac{5}{2}^-) = 0.49$  and  $0.89$   $\text{nm}^2$  for  $\beta = -0.32$  and  $0.20$ , respectively. The reduction of this transition probability for negative deformation suggests as a possible solution larger admixtures of bands with different parentage than  $f_{7/2}$  in the  $\frac{3}{2}^-$  state as can be seen from the increase of the components marked "others" in the squared amplitudes of the wave function (Fig. 4). For  $\beta = -0.32$  the closest state of this kind which can mix into the wave function is the  $\frac{3}{2}^-$  state based on Nilsson level 16. Lowering the unperturbed energy of this state will result in a larger mixing. In fact, increasing the amplitude of this state in the wave function by a factor of 2 results in a reduction of the  $M1$ -transition probability between the  $\frac{3}{2}^-$  and  $\frac{5}{2}^-$  state to a value of  $B(M1; \frac{3}{2}^- \rightarrow \frac{5}{2}^-) = 0.12$   $\text{nm}^2$ . This is mainly due to the small  $|j\Omega\rangle = |\frac{3}{2}^- \frac{3}{2}\rangle$  and  $|\frac{7}{2}^- \frac{3}{2}\rangle$  components (10% and 20%, respectively) in the single-particle wave function of Nilsson level 16. Although this value is still large, it clearly shows the sensitivity of this  $M1$  transition to this particular admixture. This change

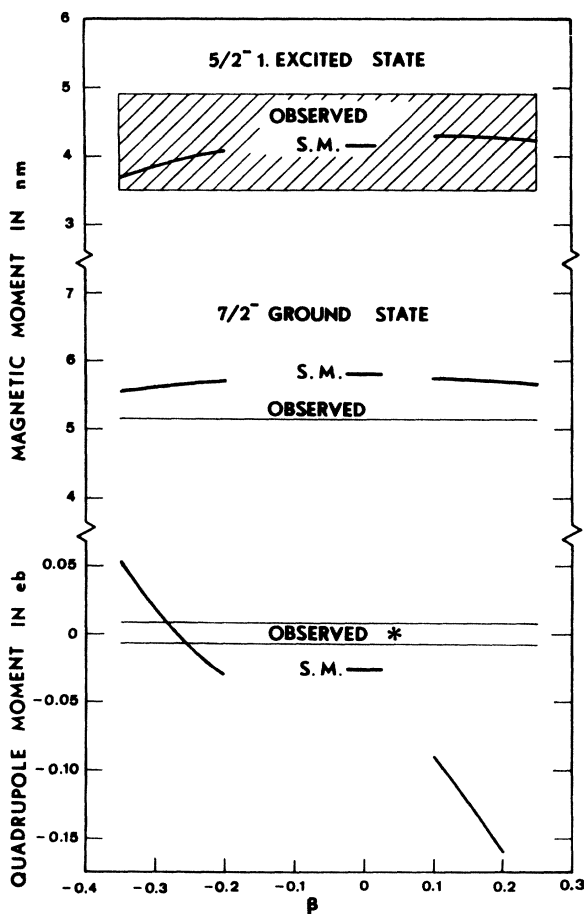


FIG. 5. The magnetic moment of the ground and the first excited state and the quadrupole moment as a function of the deformation. The shell-model values for the free proton gyromagnetic ratio and charge (S.M.) are plotted at  $\beta=0$  for comparison. \* implies that the observed quadrupole moment has been plotted both as negative and positive, since the absolute value has not been determined experimentally.

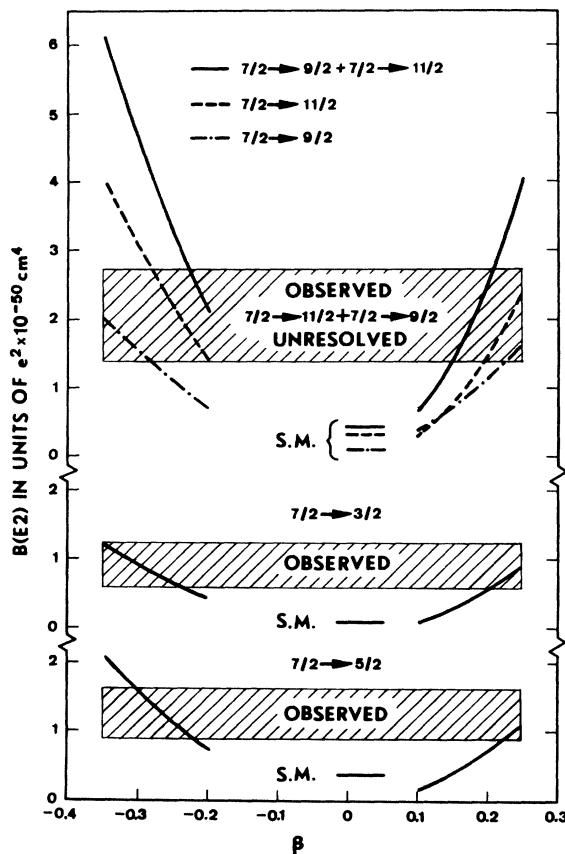


FIG. 6. Observed and calculated  $B(E2)$  transition rates. The shell-model values (S.M.), computed with the free proton charge, are plotted at  $\beta=0$  for comparison.

of the wave function decreases the  $B(E2; \frac{7}{2}^- \rightarrow \frac{3}{2}^-)$  by only 20%; all other transitions and moments remain unaffected.

## V. CONCLUSION

We find that the strong-coupling model gives us an adequate first-order representation of the energy levels, moments and transition rates in  $V^{51}$ . This result is achieved without using an effective moment or an effective charge as is necessary in the shell-model treatment. Our results favor oblate over prolate deformation. A measurement of the sign of the quadrupole moment and of the spins and de-excitation properties of the states between 2 and 3 MeV would be very helpful in clarifying this point.

## ACKNOWLEDGMENTS

We appreciate very much the constant encouragement by Professor D. A. Bromley and interesting discussions with him and Professor C. K. Bockelman. We thank also Dr. J. Weneser for stimulating discussions. The support of the U. S. Atomic Energy Commission and the National Science Foundation is gratefully acknowledged.